Assessment of salt Crystallization through numerical modelling

G. Castellazzi, S. de Miranda, L. Grementieri, L. Molari, F. Ubertini[1]

ABSTRACT

Salt crystallization is one of the major factors of degradation of porous materials such as masonry. This paper presents a coupled multiphase model for hygrothermal analysis of masonry structures and the effective prediction of stress induced by salt crystallization. The independent variables chosen to describe all the process are: the pore humidity, the concentration of dissolved salt and the temperature. The governing equations of the model are: the moisture balance equation, expressed in function of the humidity, the conservation equation for the total stored energy, the balance equation for the dissolved salt and a kinetic expression for the salt crystallization law. The model is used to simulate the results of an extensive experimental campaign carried out on a masonry wall exposed to weather conditions for four months.

Keywords

Masonry, salt crystallization, material degradation, multiphase modelling.

1. Introduction

Salt crystallization is one of the major factors of degradation of porous materials like masonry. As the water evaporates, the salt concentration of pore solution increases until salt precipitates causing the presence of efflorescence or sub-fluorescence and severe damage can result.

Since the hygrothermal conditions strongly influence the salt precipitation, an accurate transient heat, air and moisture (HAM) transfer model in porous material is essential to capture the phenomenon. To this model it is necessary to add a proper crystallization kinetics law and an effective assessment of the resultant stress on the masonry wall. The resulting model is fully coupled and very demanding from the computational point of view.

2. The model

The model presented here is the extension of the model proposed in [1]. In particular here all the dependencies of the parameters upon the temperature are taken into account and the numerical applications are performed considering the non-isothermal conditions. This is the crucial step to simulate all the types of salt even those, such as sulfates, with an evident dependency upon temperature of the crystallized salt and of the saturation value.

The masonry is described as a multiphase continuous porous medium [2],[3]. The porous medium consists of a network of interconnected voids (pores) inside a solid skeleton. The voids are assumed to be filled partly with a liquid phase, partly with a gaseous phase and partly with precipitated or crystallized salt. The effect of the deformation of the material matrix on transport of various phases is neglected. The liquid phase is an ideal solution of liquid water and dissolved salt. Only one salt is assumed to be dissolved in the solution.

All the phases and species are summarized in Table 1 with their identified symbols.

The content of each component can be described by the concentration c_α^π, defined as the mass of a in p-phase per unit volume of porous medium, or by the corresponding saturation degree S_α^π.

Table 1 Phases and species of the model.

π – Phases		α – Species	
Gaseous phase	g	Water vapour	w
Liquid phase	l	Liquid water	w
(salt solution)		Dissolved salt	s
Solid phase	s	Matrix material	m
		Precipitated salt	s

For simplicity, an instantaneous thermodynamic equilibrium is assumed between liquid phase and gaseous phase. Based on this assumption, it is convenient to combine liquid water concentration and vapour water concentration into *moisture concentration* c_w :

$$c_w = c_w^g + c_w^l$$

In order to keep the model simple, but useful, the *concentration of liquid water* can be approximated to the *concentration of moisture*:

$$c_w \cong c_w^l$$

The mathematical model presented in the following sections consists of three balance equations referring to the Representative Elementary Volume REV (moisture mass conservation, salt mass conservation and energy conservation) together with an evolution equation describing salt precipitation/dissolution kinetics. The primary variables are: the pore relative humidity h (defined as the vapour pressure over the vapour pressure at saturation, here considered dependent upon the concentration of dissolved salt and of temperature), the mass fraction of dissolved salt w and the temperature T. These independent variables are supplemented by the internal variable c_s^s which represents the concentration of crystallized salt.

1 DICAM, University of Bologna, V.le Risorgimento 2, Bologna, Italy

2.1 BALANCE EQUATIONS

Referring to a REV, at the macroscopic scale the mass conservation equations of water vapour, liquid water and salt can be written as:

$$\frac{\partial c_w^g}{\partial t} + \nabla \cdot \mathbf{j}_w^g = \mu_w^{lg}, \tag{1}$$

$$\frac{\partial c_w^l}{\partial t} + \nabla \cdot \mathbf{j}_w^l = -\mu_w^{lg} - \mu_w^{ls}, \tag{2}$$

$$\frac{\partial c_s^l}{\partial t} + \nabla \cdot \mathbf{j}_s^l + \frac{\partial c_s^s}{\partial t} = 0, \tag{3}$$

where $\mathbf{j}_w^g$ is the flux of water vapour, $\mathbf{j}_w^l$ is the flux of liquid water and $\mathbf{j}_s^l$ is the flux of dissolved salt. The source terms μ_w^{lg} and μ_w^{ls} stem from phase transition processes. In particular, μ_w^{lg} is the water evaporation rate, that is a source term in the water vapour balance equation and a sink term in the liquid water balance equation. Term μ_w^{ls} is the rate of liquid water consumed due to crystallization of hydrated salt crystals equal to 0 in the case of salt without hydrated crystal like NaCl. Finally, the last term in the third equation accounts for crystallization (dissolution) rate.

The first two equations can be added together to obtain the moisture balance equation:

$$\frac{\partial c_w}{\partial t} + \nabla \cdot \mathbf{j}_w = -\mu_w^{ls}, \tag{4}$$

with $\mathbf{j}_w = \mathbf{j}_w^g + \mathbf{j}_w^l$.

The conservation equation for the total stored energy within the REV is stated by accounting for the energy transport by conduction and transport of enthalpy associated with the mass flux of each individual component:

$$\frac{\partial e}{\partial t} + \nabla \cdot \mathbf{j}_e = 0, \tag{5}$$

with

$$e = c_m^s e_m^s + c_w^g e_w^g + c_w^l e_w^l + c_s^l e_s^l + c_s^s e_s^s, \tag{6}$$

$$\mathbf{j}_e = \mathbf{j}_q + e_w^g \mathbf{j}_w^g + e_w^l \mathbf{j}_w^l + e_s^l \mathbf{j}_s^l. \tag{7}$$

In the above expressions e is the total enthalpy per unit volume of porous medium, e_α^π is the enthalpy of α in p-phase and $\mathbf{j}_q$ is the heat flux. Notice that c_m^s is the bulk density of material matrix. For simplicity no heat source/sink is considered.

The enthalpies of various components are expressed with respect to a reference state at $T = 0$ in the following forms:

$$\begin{aligned} &e_m^s = \beta_m^s T, \quad e_w^g = \beta_w^g T + H_{eva}, \quad e_w^l = \beta_w^l T, \\ &e_s^l = \beta_s^l T, \quad e_s^s = \beta_s^s T + H_{cry}, \end{aligned} \tag{8}$$

where β_α^π is the specific heat capacity of a in p-phase, H_{eva} is the latent heat of evaporation and H_{cry} is the latent heat of crystallization.

Substituting the above expressions into eq. and making use of eqs. -

$$\begin{aligned} &\rho_{eff}\beta_{eff}\frac{\partial T}{\partial t} + \nabla \cdot \mathbf{j}_q + \\ &+ \left(\beta_w^g \mathbf{j}_w^g + \beta_w^l \mathbf{j}_w^l + \beta_s^l \mathbf{j}_s^l\right) \cdot \nabla T + \\ &- \mu_w^{lg}\left[\left(\beta_w^l - \beta_w^g\right)T - H_{eva}\right] - \mu_w^{ls}\beta_w^l T + \\ &+ \frac{\partial c_s^s}{\partial t}\left[\left(\beta_s^s - \beta_s^l\right)T + H_{cry}\right] = 0, \end{aligned} \tag{9}$$

where ρ_{eff} and β_{eff} are the effective mass density and the effective specific heat capacity of the porous medium:

$$\rho_{eff} = c_m^s + c_w^g + c_w^l + c_s^l + c_s^s, \tag{10}$$

$$\beta_{eff} = \frac{c_m^s \beta_m^s + c_w^g \beta_w^g + c_w^l \beta_w^l + c_s^l \beta_s^l + c_s^s \beta_s^s}{\rho_{eff}}. \tag{11}$$

2.2 CRYSTALLIZATION

Crystallization starts when the supersaturation ratio is greater than the threshold α_0 and dissolution starts when the supersaturation ratio is less than one:

$\omega / \omega_{sat} > \alpha_0$ crystallization

$\omega / \omega_{sat} < 1$ dissolution.

For primary crystallization $\alpha_0 > 1$, but when the first salt crystal appears in the pores, further crystallization proceeds at $\alpha_0 = 1$.

Denoting by G the growth rate of the crystal characteristic length, the following relation can be assumed according to [4]:

$$G = K_C \left| \frac{\omega}{\omega_{sat}} - 1 \right|^p, \tag{12}$$

If reference is made to a pore model, based on the idea proposed in [5] with isotropic distribution of cylindrical pores, the kinetics of crystallization can be written as:

$$\frac{\partial c_s^s}{\partial t} = n\phi_0 \left(S_w^l + S_s^l\right)\rho_s^s \left(\pi r_p^{\,2}\right) G \tag{13}$$

where r_p denotes the average pore radius, n the amount of nuclei per unit volume of solution.

When supersaturation is reached, a certain amount of stable nuclei is assumed to be present in the solution. In particular, to keep the mathematical model as simple as possible, nuclei are assumed of cylindrical form with radius r_p.

2.3 CONSTITUTIVE EQUATIONS

The following expressions are assumed as constitutive equations for the gas flow and the capillary liquid flow:

$$\mathbf{j}_w^g = -\frac{D_v}{R_v T}\nabla p_v, \tag{14}$$

$$\mathbf{j}_{ws}^l = -K_l \nabla p_c, \tag{15}$$

where D_v is the vapour permeability, K_l is the liquid conductivity of the salt solution, p_v is the vapour pressure, p_c in the capillary pressure, R_v is the gas constant of water vapour.

In particular

$$D_v = \frac{D_v^{air}}{\tau_v} f_v(S_w^g), \quad f_v = (S_w^g)^{n_g}, \tag{16}$$

where τ_v is the vapour resistance factor.

An expression of D_v^{air} can be found in [6]:

$$D_v^{air} = 2.306 \cdot 10^{-5}\left(\frac{T}{273.15}\right)^{1.81} \tag{17}$$

Regarding eq (15)

$$K_l = g_\omega(\omega) D_l f_l(S_w^l), \quad f_l = (S_w^l)^{n_l}, \tag{18}$$

where the exponent n_l ranges from 1 to 6 [4]. An empirical expression proposed in [6] for the salt-free conductivity is:

$$D_l = \left[3.8\left(\frac{A}{\phi_0 \rho_w^l}\right)^2 10^{3\left(s_w^l - 1\right)}\right]\frac{\partial c_w}{\partial h}\frac{h}{\rho_w^l R_v T}, \tag{19}$$

where A is a parameter called water adsorption coefficient.

The dependency of liquid conductivity on dissolved salt concentration in eq (18) is taken as [7]:

$$g_\omega = \frac{\rho_{ws}^l}{\rho_w^l}\left(1 - 0.03\, m\right), \tag{20}$$

where m is the molality, measured as the number of NaCl moles per kilogram of water.

The vapour pressure and the capillary pressure in eqs. (14) and (15) can be expressed in terms of relative humidity h as:

$$p_v = p_{v,sat} h, \tag{21}$$

$$p_c = \rho_w^l R_v T \ln(h), \tag{22}$$

where $P_{v,sat}$ is the saturation vapour pressure of the salt mixture, that depends on temperature as well as on dissolved salt concentration.

The $p_{v,sat}$ can be expressed as:

$$p_{v,sat} = p_{v,sat\,w}(T) \cdot a_w(\omega) \tag{23}$$

where $a_w(\omega)$ is the water activity of the salt solution, defined as:

$$a_w(\omega) = \gamma X_w, \tag{24}$$

where γ is the mean activity coefficient of the dissolved salt using the mole fraction scale:

$$X_w(\omega) = \frac{(1-\omega) M_{solute}}{(1-\omega) M_{solute} + \omega M_{H_2O}}, \tag{25}$$

where M_{solute} (g/mol) is the molar mass of the solute and M_{H_2O} (g/mol) is the molar mass of the pure water.

Ignoring, for simplicity, such a negligible value, the final expression for K_s can be taken as

$$K_s = \frac{D_s}{\tau_l} f_s(S_w^l), \quad f_s = (S_w^l)^{n_s}, \tag{26}$$

where n_s is a saturation exponent.

The heat flux is taken as

$$\mathbf{j}_q = -\lambda_{eff} \nabla T, \tag{27}$$

where λ_{eff} is the effective thermal conductivity of the porous material. It accounts for the heat conduction through the skeleton and the mobile phases. Since the thermal conductivity of a salt solution is approximately proportional to its water content, λ_{eff} can be determined based on the following relation

$$\lambda_{eff} = \lambda_m^{dry} + \phi_0\left(S_w^l \lambda_w + S_s^s \lambda_s\right). \tag{28}$$

2.3.1 Sorption/desorption curves

The analytical expression for sorption/desorption curves proposed in [6] has been considered:

$$S_{ws}^l = \frac{\psi - 1}{\psi - h} h \tag{29}$$

Where ψ is a constant experimentally tuned. To take into account the variation upon the temperature, the *modified Oswin model* is considered. In particular, ψ is considered dependent on the temperature and is obtained by fitting experimental data or the predicted data provided by the modified Oswin model by enforcing the value of water content at a certain value of relative humidity.:

$$S_{ws}^l = \frac{\psi(T) - 1}{\psi(T) - h} h\ . \tag{30}$$

2.3.2 Evaporation source term

$$\mu_w^{lg} = -\nabla \cdot \left(K_g \nabla p_v\right), \tag{31}$$

where K_g is the *vapour permeability*, which is function of the humidity h and temperature T and R_v is the *gas constant of water vapour.*

Notice that the *water evaporation rate* decreases if the relative humidity h increases.

Taking into account the dependency of $p_{v,sat}$ on T and ω, it is possible to obtain the relation between the *water evaporation rate* and the independent variables h, T, ω:

$$\mu_w^{lg} = -\left(\frac{\partial K_g}{\partial T} p_{v,sat} + 2K_g \frac{\partial p_{v,sat}}{\partial T}\right)\nabla T \cdot \nabla h$$
$$- 2K_g \frac{\partial p_{v,sat}}{\partial \omega}\nabla \omega \cdot \nabla - K_g p_{v,sat}\nabla^2 h$$
$$-\left(\frac{\partial K_g}{\partial T} h \frac{\partial p_{v,sat}}{\partial \omega} + 2K_g h \frac{\partial^2 p_{v,sat}}{\partial \omega \partial T}\right)\nabla \omega \cdot \nabla T +$$
$$- K_g h \frac{\partial^2 p_{v,sat}}{\partial \omega^2}\nabla \omega \cdot \nabla \omega +$$
$$-\left(\frac{\partial K_g}{\partial T} h \frac{\partial p_{v,sat}}{\partial T} + K_g h \frac{\partial^2 p_{v,sat}}{\partial T^2}\right)\nabla T \cdot \nabla T$$
$$-\left[K_g h \frac{\partial p_{v,sat}}{\partial T}\nabla^2 T + K_g h \frac{\partial p_{v,sat}}{\partial \omega}\nabla^2 \omega\right],$$

where

$$K_g = \frac{D_v}{R_v T}.$$

2.4 STRESS PREDICTION

A growing crystal causes a pressure on the pores of a porous material which contains it. In particular, the pressure which a growing crystal can exercise depends on the degree of supersaturation.

The expression for the crystallization pressure proposed in [8] is used. In this expression, the capability of a growing crystal to exert pressure against its confining 'environment' is given as a function of the supersaturation ratio of the solution as follows:

$$p_s = \frac{\nu RT}{V_s}\left(\ln\frac{\omega}{\omega_{sat}} + \ln\frac{\gamma}{\gamma_{sat}} + \frac{\nu_0}{\nu}\ln\frac{a_w}{a_{w\,sat}}\right) \quad (32)$$

where R is the ideal gas constant (8.31 10^{-3} kJ/mol/K), p_s is the pressure exerted by the growing crystal, V_s the molar volume of the precipitated salt, ν the total number of ions released upon complete dissociation of the salt, ν_0 number of water molecules per salt mole which is null for non-hydrated salts and γ the mean activity coefficient that can be evaluated by the ion interaction approach as illustrated in [8] and in [9].

The total number of ions released upon complete dissociation of the salt ν is an integer number equal 2 for 1-1 salts like NaCl and equal 3 for 2-1 salts like Na_2SO_4.

Under the hypothesis of *ideal solution* $\gamma=\gamma_{sat}=1$ and non-hydrated salts it leads to:

$$p_s = \frac{\nu RT}{V_s}\left(\ln\frac{\omega}{\omega_{sat}}\right) \quad (33)$$

A salt crystal keeps growing until the side of the crystal which undergoes the pressure remains in contact with a supersaturated solution. The higher the pressure exerted, the higher the salt concentration needed for the process to continue.

The crystallization pressure plays a crucial role in the damage process of the porous material.

For a more accurate prediction of damage, it is necessary to determine the macroscopic stress based on the microscopic distribution of the crystallization pressure within the pores.

The simplest upscaling procedure is adopted to estimate the induced tensile stress at macroscopic scale:

$$\sigma_0 = S_s^s p_s \quad (34)$$

Note that, as expected, the stress depends upon the amount of precipitated salt. Although very simple, Eq. (34) permits a satisfactory prediction of damage onset, as shown in [1].

2.5 MODEL EQUATIONS

Taking into account the dependency on temperature of $S_{ws}^{\ l} = S_{ws}^{\ l}(h, \omega, T)$, and the contribution of effective porosity f_{eff}, the moisture content c_w is a function of all the independent variables:

$$c_w = c_w(h, \omega, T, c_s^s) \quad (35)$$

Considering also the dependency of saturation vapour pressure of the salt mixture $p_{v,sat}$ on temperature T and on dissolved salt concentration ω:

$$p_{v,sat} = p_{v,sat}(\omega, T) \quad (36)$$

and the dependency of H_{eva} and H_{cry} on temperature, the resulting governing equations of the model, can be written as:

$$\varphi_h \frac{\partial h}{\partial t} + \nabla \cdot \left[-C_{hh}\nabla h - C_{hT}\nabla T - C_{h\omega}\nabla \omega\right] +$$
$$\varphi_{h\omega}\frac{\partial \omega}{\partial t} + \varphi_{hT}\frac{\partial T}{\partial t} + \varphi_{hs}\frac{\partial c_s^s}{\partial t} + \mu_w^{ls} = 0, \quad (37)$$

(38)

$$\varphi_\omega \frac{\partial \omega}{\partial t} + \nabla \cdot \left[-C_{\omega h}\nabla h - C_{\omega T}\nabla T - C_{\omega\omega}\nabla \omega\right]$$
$$+ \varphi_{\omega h}\frac{\partial h}{\partial t} + \varphi_{\omega T}\frac{\partial T}{\partial t} + \varphi_s \frac{\partial c_s^s}{\partial t} = 0,$$

$$\varphi_T \frac{\partial T}{\partial t} + \nabla \cdot \left[-C_{TT}\nabla T - C_{Th}\nabla h - C_{T\omega}\nabla \omega\right] + \quad (39)$$
$$\varphi_{Ts}\frac{\partial c_s^s}{\partial t} - \mu_w^{ls} B_w^* + \mu_w^{lg} B_w = 0$$

$$\frac{\partial c_s^s}{\partial t} = \pm C_{ss}\left|\frac{\omega}{\omega_{sat}} - 1\right|^p. \quad (40)$$

The expressions of coefficients φ_i, C_{ij}, B_i are detailed for the equation (37):

$$\varphi_h = \frac{\partial c_w}{\partial h},\ \varphi_{h\omega} = \frac{\partial c_w}{\partial \omega},$$

$$\varphi_{hT} = \frac{\partial c_w}{\partial T},\ \varphi_{hs_i} = \frac{\partial c_w}{\partial c^s_{s_i}},$$

$$C_{hh} = \frac{D_v}{R_v T} p_{v,sat} + (1-\omega)\frac{\rho^l_w R_v T K_l}{h}$$

$$C_{hT} = \frac{D_v h}{R_v T}\frac{\partial p_{v,sat}}{\partial T} + (1-\omega)\rho^l_w R_v K_l \ln(h),$$

$$C_{h\omega} = \frac{D_v h}{R_v T}\frac{\partial p_{v,sat}}{\partial \omega} - \rho^l_{ws} K_s.$$

for the equation (38)

$$\varphi_\omega = \frac{c_w}{(1-\omega)^2} + \frac{\omega}{1-\omega}\varphi_{h\omega},\quad \varphi_{\omega h} = \frac{\omega}{1-\omega}\varphi_h,$$

$$\varphi_{\omega T} = \frac{\omega}{1-\omega}\varphi_{hT},\quad \varphi_s = 1 + \frac{\omega}{1-\omega}\varphi_{hs_i}$$

$$C_{\omega\omega} = \rho^l_{ws} K_s,$$

$$C_{\omega h} = \omega\frac{\rho^l_w R_v T K_l}{h},$$

$$C_{\omega T} = \omega\rho^l_w R_v T K_l \ln(h).$$

for the equation (39):

$$C_{TT} = \lambda_{eff} + \left(\beta^g_w T + H_{eva}\right)\frac{D_v h}{R_v T}\frac{\partial p_{v,sat}}{\partial T}$$
$$+ \left(\beta^l_w(1-\omega) + \beta^l_s \omega\right)\rho^l_w R_v K_l \ln(h)T$$

$$C_{Th} = \left(\beta^g_w T + H_{eva}\right)\frac{D_v}{R_v T} p_{v,sat}$$
$$+ \left(\beta^l_w(1-\omega) + \beta^l_s \omega\right)\frac{\rho^l_w R_v T^2 K_l}{h}$$

$$C_{T\omega} = \left(\beta^g_w T + H_{eva}\right)\frac{D_v h}{R_v T}\frac{\partial p_{v,sat}}{\partial \omega}$$
$$+ \left(\beta^l_s - \beta^l_w\right)\rho^l_{ws} K_s T$$

$$B_w = \left(\beta^g_w - \beta^l_w\right)T + H_{eva}$$

$$B^*_w = \beta^l_w T$$

$$\varphi_T = \beta_{eff}\rho_{eff}$$

Finally, coefficients of the kinetic equations (40) are:

$$C_{ss} = S^l_{ws}\left(n\phi_0\rho^s_s\pi r^2_p\right)K_C.$$

2.6 Boundary conditions

The *model equations* should be completed by introducing *initial and boundary conditions*. In particular, the boundary conditions on a certain portion of the domain boundary can be of the *Dirichlet* type:

$$h = \overline{h} \qquad \omega = \overline{\omega} \qquad T = \overline{T}$$

and of *Neumann's* or *Robin's* type:

$$\mathbf{j}_w \cdot \mathbf{n} = q_w + \gamma_w(h - h_\alpha), \qquad \mathbf{j}^l_s \cdot \mathbf{n} = q_\omega,$$
$$\mathbf{j}_e \cdot \mathbf{n} = q_T + \gamma_T(T - T_\alpha),$$

where $\mathbf{n}$ is the *outward unit vector normal to the boundary*, $\overline{h}, \overline{\omega}$ and $\overline{T}$ are the prescribed humidity, salt concentration and temperature, respectively, q_w, q_ω and q_T are the prescribed normal fluxes of moisture, salt and heat, h_α and T_α are the prescribed environmental humidity and temperature, and γ_w and γ_T are the convective humidity and thermal coefficients, respectively.

As expressed in [10] from the external temperature on the right side of the wall equal to the left one, it is possible to write the *convective heat transfer coefficient* γ_T as:

$$\gamma_T = \frac{\lambda_{eff}}{s} \qquad (2)$$

where s in the *thickness of the wall in the flux direction considered.*

3. Numerical application

To demonstrate the effectiveness of the present approach, a masonry wall exposed for four months to outdoor conditions was used to predict the variation of moisture content, salt transport and stress due to salt crystallization. The geometry of the investigated masonry wall is shown in Figure 1. The wall was built in outdoor conditions in July 2010, with the base exposed to a solution of water and NaCl with a concentration equal to 0.05% $kg_{salt}/kg_{solution}$ for four months.

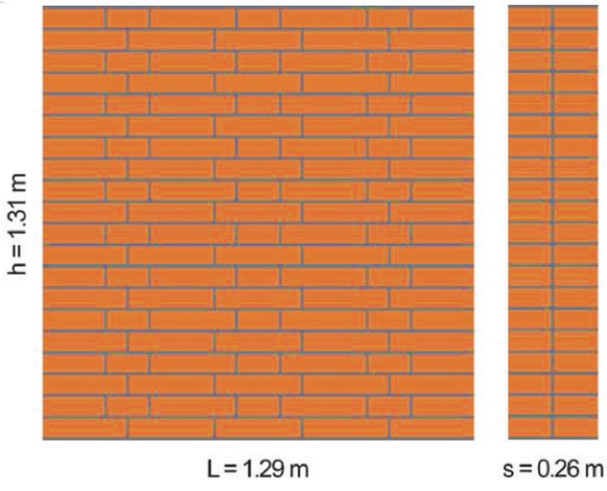

Figure 1. Geometry of the masonry wall considered.

The typical element size of finite mesh is 2.6 cm. Lagrangian quadratic finite elements were chosen. The wall was modeled as though made of a single material, using the material parameters calibrated in [1] for the equivalent brick. The boundary conditions are taken as:

- $h = 1.0$ and $\omega = 0.0005$ at the base when this is immersed in the solution of water and NaCl;

- $\mathbf{j}_w \cdot \mathbf{n} = \gamma_w (h - h_\alpha)$ and $\mathbf{j}_\omega \cdot \mathbf{n} = 0$ on the sides where h_α varies in time according to the environmental humidity measured in Bologna in the period July 2010-October 2010 (as drawn in Figure 2), and $\gamma_w = 0.4$ kg/m²/s;

- $\mathbf{j}_q \cdot \mathbf{n} = \gamma_T (T - T_\alpha)$ at the sides where T_α varies in time according to the environmental humidity measured in Bologna in the period July 2010-Sep 2010 (as drawn in Figure 2).

- $\mathbf{j}_w \cdot \mathbf{n} = 0$ and $\mathbf{j}_\omega \cdot \mathbf{n} = 0$ on the top face and at the base when this is laid over the water proof layer.

In Figure 3 and 4 the results of the numerical simulations of the wall exposed to outdoor condition in the period July 2010-October 2010 in non-isothermal regime after 15, 30, 45 and 60 days are depicted, representing humidity, temperature, dissolved and precipitated salts, respectively.

The pictures at different times show the time evolution of the variables. From the map of the humidity in Figure (3) the rising height of the liquid water is clearly visible .

From Figure 4 it can be noted that the higher values of the dissolved salt are in the zones just over the water front, towards the external surfaces. It can be noted as it is in these zones the salt starts to crystallize.

Comparing the results of Figure 3 and 4 with the results obtained in the same simulation in isothermal regime (and neglecting the dependency of the saturation vapour pressure on dissolved salt concentration) in [1], it can be noted as the same order of magnitude of the amount of precipitated salt is obtained even though with a value which has almost doubled, while the patterns of crystallized salts are similar.

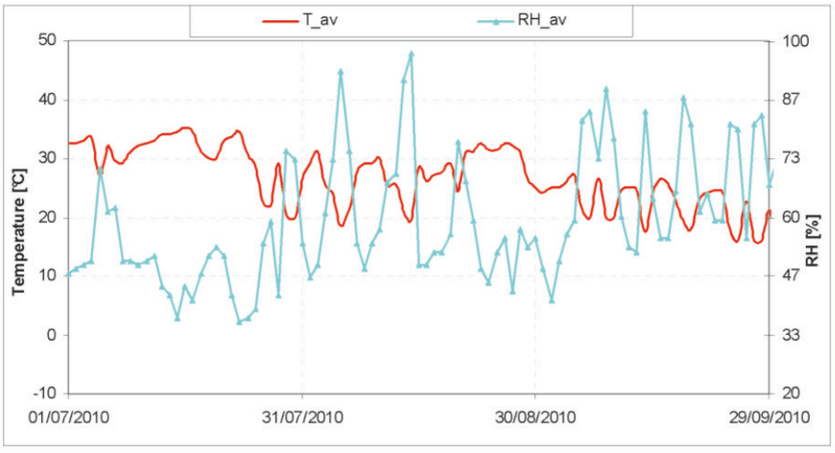

Figure 2. Humidity and temperature average in Bologna from July to October 2010. These data are from a metereological station near the Lab.

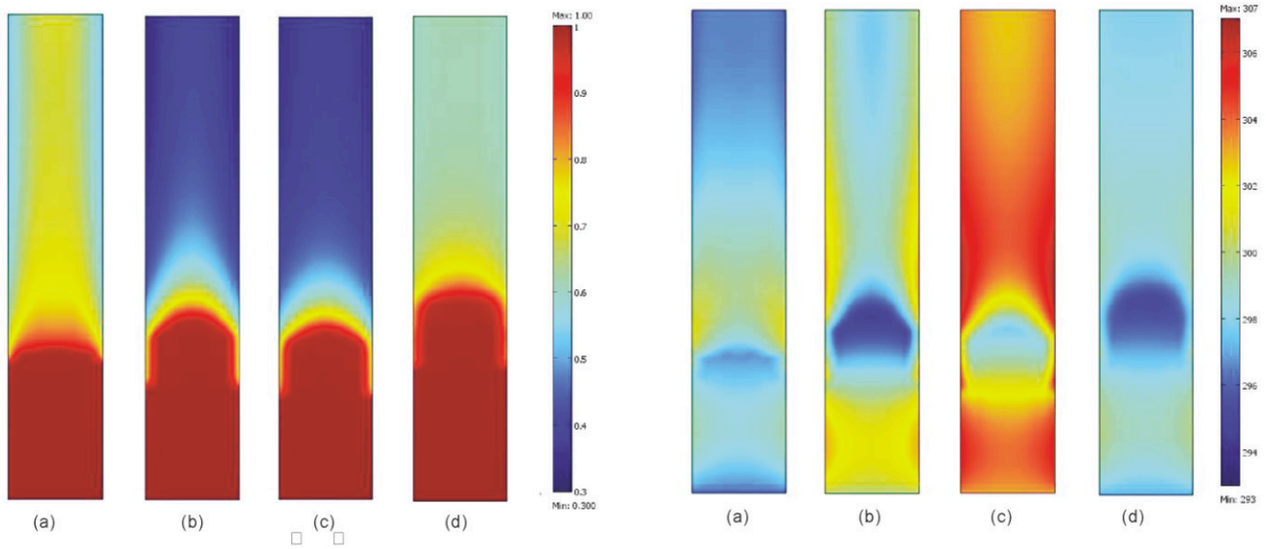

Figure 3. Maps of temperature of humidity (on the left) and temperature (on the right) after 15 (a), 30(b), 45(c) and 60(d) days.

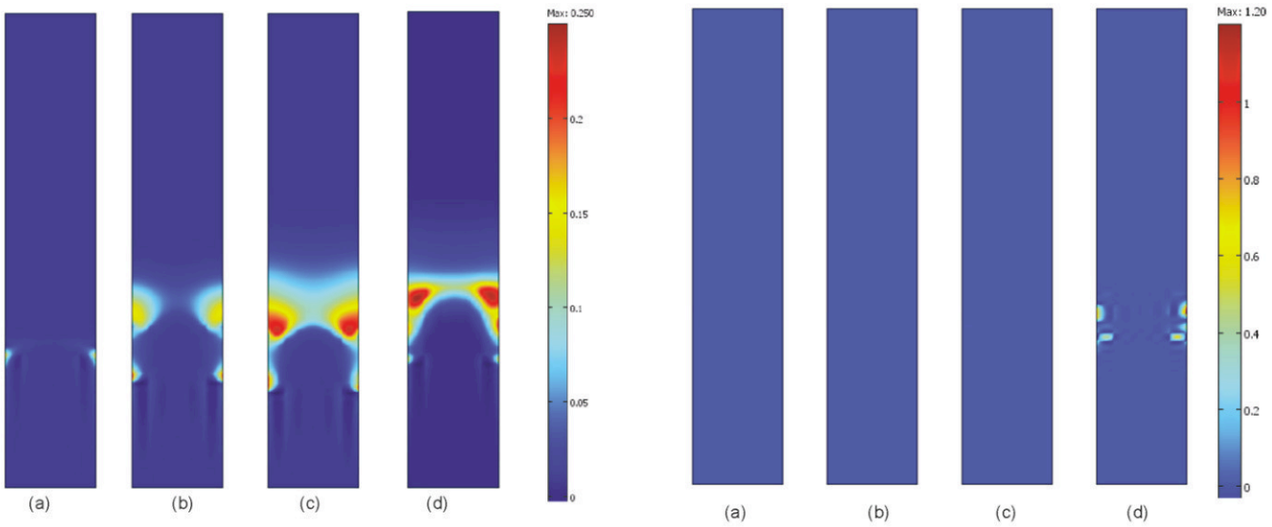

Figure 4. Maps of temperature of dissolved salt (on the left) and of crystallized salt (on the right) after 15 (a), 30(b), 45(c) and 60(d) days.

4. Conclusions

The model proposed here is a fully coupled model able to predict crystallization patterns by taking into account non-isothermal conditions. The effectiveness of the approach is demonstrated through the very demanding numerical simulations of an experimental test in outdoor conditions.

5. References

[1] Castellazzi G., Colla C., de Miranda S., Formica G., Gabrielli E., Molari L., Ubertini F., 2013, A coupled multiphase model for hygrothermal analysis of masonry structures and prediction of stress induced by salt crystallization. Construction and Building Materials, 41: 717-731.

[2] Schrefler BA. Mechanics and thermodynamics of saturated/unsaturated porous materials and quantitative solutions. Applied Mechanics Review 2002; 55:351-389.Gawin and Schrefler 1996

[3] Gawin D, Schrefler BA. Thermo-hydro-mechanical analysis of partially saturated porous materials. Eng. Comput. 1996; 13:113–143.

[4] Koniorczyk M, Gawin D. Numerical modelling of salt transport and precipitation in nonisothermal partially saturated porous media considering kinetics of salt phase changes. Transport in Porous Media 2011; 87:57-76.

[5] Espinosa RM, Franke L, Deckelmann G. Phase changes of salts in porous materials crystallization, hydration and deliquescence. Construction and Building Materials 2008; 22:1758-1773

[6] Sykora J, Krejci T, Sejnoha M. Computational homogenization of non-stationary transport processes in masonry structures. Journal of Computational and Applied Matematics 2012; 236:4745-4755.

[7] Nicolai A. Modeling and numerical simulation of salt transport and phase transitions in unsaturated porous building materials. Ph. D. dissertation, Syracuse University, New York, 2007.

[8] Steiger M. Crystal growth in porous materials - I: The crystallization pressure of large crystals. Journal of Crystal Growth 2005; 282:455-469

[9] Steiger, M., Kiekbusch J., Nicolai A., An improved model incorporating Pitzer's equations for calculation of thermodynamic properties of pore solutions implemented into an efficient program code, Construction and Building Materials, 2008; 22 : 1841–1850.

[10] Kranjc T., Peternelj J., Kozak J., The rate of heat flow through a flat vertical wall due to conjugate heat transfer, International Journal of Heat and Mass Transfer, Volume 53, Issues 5–6, February 2010, Pages 1231-1236